

Probabilistic inverse optimal control with local linearization for non-linear partially observable systems

Dominik Straub*, Matthias Schultheis*, Heinz Koepl, and Constantin A. Rothkopf

Centre for Cognitive Science, Technical University of Darmstadt, Darmstadt, Germany

Abstract

Inverse optimal control methods can be used to characterize behavior in sequential decision-making tasks. Most existing work, however, requires the control signals to be known, or is limited to fully-observable or linear systems. This paper introduces a probabilistic approach to inverse optimal control for stochastic non-linear systems with missing control signals and partial observability that unifies existing approaches. By using an explicit model of the noise characteristics of the sensory and control systems of the agent in conjunction with local linearization techniques, we derive an approximate likelihood for the model parameters, which can be computed within a single forward pass. We evaluate our proposed method on stochastic and partially observable version of classic control tasks, a navigation task, and a manual reaching task. The proposed method has broad applicability, ranging from imitation learning to sensorimotor neuroscience.

1 Introduction

Inverse optimal control (IOC) is the problem of inferring an agent’s cost function, and possibly other properties of their internal model, from observed behavior. While IOC has been a fundamental task in artificial intelligence, optimal control, and machine learning, particularly reinforcement learning and robotics, it has widespread applicability in several scientific fields including behavioral economics, psychology, and neuroscience. For example, in cognitive science and sensorimotor neuroscience optimal control models have been able to explain key properties of behavior, such as speed-accuracy trade-offs (Harris and Wolpert, 1998) or the minimum intervention principle (Todorov and Jordan, 2002). But, while researchers usually build an optimal control model and compare its predictions

to behavior, certain parameters of the agent’s internal processes are typically unknown. For example, an agent might experience intrinsic costs of behavior such as effort that are different between individuals. Inferring these parameters from observed behavior can help to understand the agent’s goals, internal tradeoffs, cognitive processes and predict their behavior under novel conditions. Applying IOC in these sensorimotor control domains poses several challenges that make most previous methods not viable.

First, most IOC methods assume the agent’s action signals to be known. This assumption, while convenient in simulations or robotics applications, where the control signals may be easily quantified, does not hold in many other real-world applications. In transfer learning or behavioral experiments, the action signals are internal quantities of an animal or human, e.g., neural activity or muscle activations, and are therefore not straightforwardly observable. Thus, it is worthwhile to consider the scenario where a researcher has observations of the system’s state only, i.e., measurements of the animal’s behavior.

Second, with few exceptions (e. C.g. Chen and Ziebart, 2015; Kwon et al., 2020), IOC methods do not account for partial observability from the agent’s perspective and model the variability of the agent using a maximum causal entropy formulation (MCE; Ziebart et al., 2010). However, many real world control problems involve sensory uncertainty, which makes the state of the world partially observable and therefore contributes to the agent’s stochasticity. As an example, in sensorimotor neuroscience the noise or uncertainty in the sensory system can be well described quantitatively so that accurate observation models can be formulated, which are helpful to understand the variability of behavior (Wolpert and Ghahramani, 2000).

Third, many IOC methods are based on matching feature expectations of the cost function between the model and observed data (e.g. Ziebart et al., 2010), and are thus not easily adapted to infer parameters of other parts of the model. The cost function is often not the only quantity of interest in a behavioral experiment,

*Equal contribution

Correspondence to: Dominik Straub <dominik.straub@tu-darmstadt.de>, Matthias Schultheis <matthias.schultheis@tu-darmstadt.de>.

where researchers might be interested in also inferring the noise characteristics of the motor system or other properties of the agent’s internal model (e.g. Golub et al., 2013).

Fourth, in many real-world scenarios, the problem is not well modeled with linear dynamics and Gaussian noise, which would allow applying linear quadratic Gaussian (LQG) control (Anderson and Moore, 1990). First, the dynamics of the system may be non-linear. A common example comes from robotics and motor control, where joint angles in a kinematic chain need to be controlled and the physical system’s dynamics involve inertia, centripetal, and Coriolis forces, as well as friction and torque in the joints. Secondly, the stochasticity of the system may not be well captured by normal distributions. A prime example is biological sensorimotor control, where the system is not only non-linear but both the sensory and action noise distributions are additionally signal dependent, i.e. the variability of sensory and control signals scale with their respective means. While iterative methods for solving the optimal control problem exist (Todorov and Li, 2005), here we consider the corresponding inverse problem.

To address these issues, we adopt a probabilistic perspective of the IOC problem. We distinguish between the control problem faced by the agent and the inference problem the researcher has to solve. From the agent’s perspective, the problem consists of acting in a partially observable Markov decision process (POMDP), for which the probabilistic graphical model is shown in Figure 1, left. We consider the setting of continuous states and actions, stochastic non-linear dynamics, partial observations, and finite horizon. For this setting, there are efficient approximately optimal solutions to the estimation and control problem, for which we give an overview in Section 2. The researcher, on the other hand, is interested in inferring properties of the agent’s model and cost function. The IOC problem from their perspective can also be formulated using a probabilistic graphical model (Figure 1, right), in which the state of the system is observed, while quantities internal to the agent are latent variables.

Here, we unify MCE models, which are agnostic regarding the probabilistic structure causing the observed stochasticity of the agent’s policy, with IOC methods, which involve an explicit observation model. We allow for both: We employ an explicit observation model, but also allow the agent to have additional stochasticity through a MCE policy. We provide a solution to the IOC problem in this setting by approximate filtering of the agent’s state estimate via local linearization, which allows marginalizing over these latent variables and deriving an approximate likelihood function for observed trajectories given parameters (Section 3). This

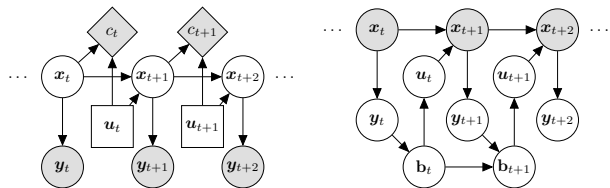


Figure 1: **Left:** Decision network from the agent’s perspective (following the notational convention used in Kochenderfer et al., 2022). At each time step t , the agent receives a partial or noisy observation y_t of the actual state x_t . The agent performs an action u_t and incurs a cost c_t . **Right:** Probabilistic graphical model from the researcher’s perspective, who observes a trajectory $x_{1:T}$ from an agent. Quantities that are internal to the agent, i.e., their partial observations y_t , their internal beliefs b_t and the action signals u_t are not directly observed.

function can be efficiently evaluated as it consists of a single forward pass. An estimate of the optimal parameters can then be determined using a gradient-based optimizer, maximizing the approximate likelihood. We evaluate our proposed method on two classical control tasks, pendulum and cartpole, as well as a navigation task, and a manual reaching task (Section 4).

Related work

Inferring costs or utilities from behavior has been of interest for a long time in several scientific fields, such as behavioral economics, psychology, and neuroscience (Mosteller and Noguee, 1951; Kahneman and Tversky, 1979; Körding and Wolpert, 2004). More specific to the problem formulation adopted here, estimating objective functions in the field of control was first investigated by Kalman (1964) in the context of deterministic linear systems with quadratic costs. More recent formulations were developed first for discrete state and action spaces under the term inverse reinforcement learning (IRL; Ng et al., 2000; Abbeel and Ng, 2004), including formulations allowing for stochasticity in action selection (Rothkopf and Dimitrakakis, 2011). In this line, the maximum entropy (ME; Ziebart et al., 2008) and MCE formulation (Ziebart et al., 2010) gave rise to a whole string of new methods, such as addressing the IOC problem for non-linear continuous systems via linearization (e.g. Levine and Koltun, 2012) or importance sampling (Boularias et al., 2011) for the case of deterministic dynamics and full observability.

IOC methods for stochastic systems have been developed that considered the setting of affine control dynamics (Aghasadeghi and Bretl, 2011; Li et al., 2011).

Arbitrary non-linear stochastic dynamics in the infinite horizon setting have been approached using model-free deep MCE IRL formulations (Finn et al., 2016; Garg et al., 2021). The latter approaches, however, yield no interpretable representation as the reward function is represented as a neural network. The partially observable setting for IOC has previously been addressed in the case of deterministic dynamics for the discrete state-action space (Choi and Kim, 2011) and continuous state, discrete action space (Silva et al., 2019). Schmitt et al. (2016) addressed systems with linear dynamics and continuous controls for a linear switching observation model. Other work has considered partial observability from the researcher’s perspective, e.g., through occlusions (Kitani et al., 2012; Bogert et al., 2016). There are some IOC methods which are applicable to partially observable and stochastic systems: Linear-quadratic-Gaussian systems have been regarded by Schultheis et al. (2021), while the work of Chen and Ziebart (2015) can be used to estimate cost functions that depend on the state only. Non-linear dynamics in the infinite-horizon setting have been approached by Kwon et al. (2020) by training a policy network as a function of the whole parameter space. This work, however, also assumes the action signals to be given and a stationary policy.

Applications where IOC methods have been used to estimate cost functions range from human locomotion (Mombaur et al., 2010) over spatial navigation (Rothkopf and Ballard, 2013), table tennis (Muelling et al., 2014), to attention switching (Schmitt et al., 2017), and target tracking (Straub and Rothkopf, 2022). Other work has been aimed at inferring other properties of control tasks, e.g. learning the dynamics model (Golub et al., 2013), learning rules (Ashwood et al., 2020), or discount functions (Schultheis et al., 2022). Several subfields of robotics including imitation and apprenticeship learning (Taylor and Stone, 2009) as well as transfer learning (Osa et al., 2018) have also employed IOC.

2 Background

Before we introduce our probabilistic approach to inverse optimal control, we give an overview of the control and filtering problems faced by the agent and algorithms that can be used to solve it. For a summary of our notation in this paper, see Appendix A.

2.1 Partially observable Markov decision processes

We consider a special case of partially observable Markov decision processes Åström (1965); Kaelbling et al. (1998), a discrete-time stochastic non-linear dynamical system (Figure 1, left) with states $\mathbf{x}_t \in \mathbb{R}^n$ following the dynamics equation $\mathbf{x}_{t+1} = f(\mathbf{x}_t, \mathbf{u}_t, \mathbf{v}_t)$, where $f : \mathbb{R}^n \times \mathbb{R}^u \times \mathbb{R}^v \rightarrow \mathbb{R}^n$ is the dynamics function, $\mathbf{u}_t \in \mathbb{R}^u$ are the controls and $\mathbf{v}_t \sim \mathcal{N}(0, I)$ is v -dimensional Gaussian noise. We assume that the agent has only partial observations $\mathbf{y}_t \in \mathbb{R}^m$ following $\mathbf{y}_t = h(\mathbf{x}_t, \mathbf{w}_t)$, with $h : \mathbb{R}^n \times \mathbb{R}^w \rightarrow \mathbb{R}^m$ the stochastic observation function and $\mathbf{w}_t \sim \mathcal{N}(0, I)$ w -dimensional Gaussian noise. While \mathbf{v}_t and \mathbf{w}_t are defined as standard normal random variables, the system can incorporate general control- and state-dependent noises through non-linear transformations within the dynamics function f and observation function h . The agent’s goal is to minimize the expected cost over a time horizon $T \in \mathbb{N}$, defined by $J = \mathbb{E}[c_T(\mathbf{x}_T) + \sum_{t=1}^{T-1} c_t(\mathbf{x}_t, \mathbf{u}_t)]$, consisting of a final state cost $c_T(\mathbf{x}_T)$ and a cost at each time step $c_t(\mathbf{x}_t, \mathbf{u}_t)$.

2.2 Iterative linear quadratic Gaussian

The fully-observable control problem analogous to Section 2.1, where we assume that the agent acts directly on the state, can be solved approximately using the method of iterative linear quadratic Gaussian (iLQG; Todorov and Li, 2005). This method iteratively linearizes the dynamics and employs a quadratic approximation of the costs around a nominal trajectory, $\{\bar{\mathbf{x}}_i, \bar{\mathbf{u}}_i\}_{i=1, \dots, T}$, with $\bar{\mathbf{x}}_i \in \mathbb{R}^n$, $\bar{\mathbf{u}}_i \in \mathbb{R}^u$, and computes the optimal linear control law, $\mathbf{u}_t = \pi_t(\mathbf{x}_t) = L_t(\mathbf{x}_t - \bar{\mathbf{x}}_t) + \mathbf{m}_t + \bar{\mathbf{u}}_{1:T}$ for the approximated system. The quantities L_t and \mathbf{m}_t are the control gain and offset, respectively, and determined through a backward pass for the current reference trajectory. In the following iteration, the determined optimal control law is used to generate a new reference trajectory and the process is repeated until the controller converges.

2.3 MCE reinforcement learning

The MCE reinforcement learning is to minimize the expected cost as in Section 2.2, while maximizing the conditional entropy of the applied stochastic policy $\Pi_t(\mathbf{u}_t | \mathbf{x}_t)$, i.e., to minimize $\mathbb{E}[J(\mathbf{x}_{1:T}, \mathbf{u}_{1:T}) - \sum_{t=1}^{T-1} H(\Pi_t(\mathbf{u}_t | \mathbf{x}_t))]$. This formulation has been used to formulate reinforcement learning as a probabilistic inference problem (Kappen et al., 2012; Toussaint, 2009; Levine, 2018) and for inverse reinforcement learning (IRL) to model the stochasticity of the agent (e.g.,

Ziebart et al., 2008, 2010). The objective of IRL is formulated as maximizing the likelihood of given states and actions $\{\mathbf{x}_t, \mathbf{u}_t\}_{t=1, \dots, N}$, induced by the maximum entropy policy $\Pi_t(\mathbf{u}_t | \mathbf{x}_t)$.

It can be shown that the resulting optimal policy is given by the distribution $\Pi_t(\mathbf{u}_t | \mathbf{x}_t) = \exp(Q_t(\mathbf{x}_t, \mathbf{u}_t) - V_t(\mathbf{x}_t))$, where Q_t is the soft Q-function at time t , given by $Q_t(\mathbf{x}_t, \mathbf{u}_t) = -c_t(\mathbf{x}_t, \mathbf{u}_t) - \mathbb{E}[V_{t+1}(\mathbf{x}_{t+1})]$ and V_t the normalization, i.e., $V_t(\mathbf{x}_t) = \log \int_{\mathbf{u}_t} \exp(Q_t(\mathbf{x}_t, \mathbf{u}_t)) d\mathbf{u}_t$ (Gleave and Toyer, 2022). For general dynamics and reward functions, it is hard to compute the soft Q-function exactly. Approximate solutions have been derived using linearization (Levine and Koltun, 2012) or importance sampling (Boularias et al., 2011). For the case of linear dynamics and quadratic reward, the optimal policy is given by a Gaussian distribution $\Pi_t(\mathbf{u}_t | \mathbf{x}_t) = \mathcal{N}(\mathbf{u}_t; L_t \mathbf{x}_t, -L_t)$, where L_t is the controller gain of the LQG controller (Levine and Koltun, 2013). This formulation can be extended to non-linear systems by using the control law in conjunction with the iLQG method (Section 2.2).

2.4 Extended Kalman filter

Given the system defined in Section 2.1, the optimal filtering problem is to compute a belief distribution of the current state given past observations, i.e., $p(\mathbf{x}_t | \mathbf{y}_{1:t-1})$. For linear-Gaussian systems, the solution is given in closed form and known as the Kalman filter (Kalman, 1960). In case of non-linear systems as in Section 2.1, a Gaussian approximation to the optimal belief can be computed using the extended Kalman filter via $\mathbf{b}_{t+1} = f(\mathbf{b}_t, \mathbf{u}_t, 0) + K_t(\mathbf{y}_t - h(\mathbf{b}_t, 0))$, where $\mathbf{b}_t \in \mathbb{R}^n$ denotes the mean of the Gaussian belief $p(\mathbf{x}_t | \mathbf{y}_1, \dots, \mathbf{y}_{t-1})$. The matrix K_t denotes the Kalman gain for time t and is computed by applying the Kalman filter to the system locally-linearized around the nominal trajectory obtained by the approximate optimal control law of iLQG (Section 2.2).

3 Probabilistic IOC

We consider an agent acting in a partially observable Markov decision process as introduced in Section 2.1. We assume that the agent acts at time t based on their belief \mathbf{b}_t about the state of the system \mathbf{x}_t , which evolves according to $\mathbf{b}_{t+1} = \beta_t(\mathbf{b}_t, \mathbf{u}_t, \mathbf{y}_t)$. While the belief of the agent is defined commonly as a distribution over the true state, here we model \mathbf{b}_t as a finite-dimensional summary statistics of the distribution, i.e., $\mathbf{b}_t \in \mathbb{R}^b$. The function $\beta_t : \mathbb{R}^b \times \mathbb{R}^u \times \mathbb{R}^m \rightarrow \mathbb{R}^b$ is called belief dynamics. We further assume that the agent follows a time-dependent policy $\pi_t : \mathbb{R}^b \times \mathbb{R}^j \rightarrow \mathbb{R}^u$, i.e., $\mathbf{u}_t =$

$\pi_t(\mathbf{b}_t, \boldsymbol{\xi}_t)$, which can be stochastic with $\boldsymbol{\xi}_t \sim \mathcal{N}(0, I)$. Note that both the belief dynamics and the policy can be time-dependent.

In the inverse optimal control problem, the goal is to estimate parameters $\boldsymbol{\theta} \in \mathbb{R}^p$ of the agent’s optimal control problem given the model and trajectory data. These parameters can include properties of the agent’s cost function, the sensory and control systems of the agent, or the system’s dynamics. We follow a probabilistic approach to inverse optimal control, i.e., we consider the likelihood function

$$p(\mathbf{x}_{1:T} | \boldsymbol{\theta}) = p(\mathbf{x}_0 | \boldsymbol{\theta}) \prod_{t=0}^{T-1} p(\mathbf{x}_{t+1} | \mathbf{x}_{1:t}, \boldsymbol{\theta}), \quad (1)$$

describing the probability of the observed trajectory data $\mathbf{x}_{1:T} := \{\mathbf{x}_t\}_{t=1, \dots, T}$ given the parameters. For a set of trajectories we assume them to be independent given the parameters so that the likelihood factorizes into single trajectory likelihoods of the form in Equation (1). In this equation, generally, each state \mathbf{x}_{t+1} depends on all previous states $\mathbf{x}_1, \dots, \mathbf{x}_t$, because the agent’s internal noisy observations and control signals are not accessible to the researcher (Figure 1, right). Therefore, the Markov property does not hold from the researcher’s perspective, rendering computation of the likelihood function intractable. To deal with this problem, we employ two key insights: First, the joint dynamical system of the states and the agent’s belief is Markovian (Van Den Berg et al., 2011). Second, by keeping track of the distribution over the agent’s belief, i.e., by performing belief tracking (Schultheis et al., 2021), we can iteratively compute the individual factors of the likelihood function in Equation (1).

We first introduce a general formulation of the IOC likelihood involving marginalization over the agent’s internal beliefs in Section 3.1. Then, we show how to make the computations tractable by local linearization in Section 3.2. In Section 3.3, we provide details for suitable linearization points, which enables us to evaluate the approximate likelihood within a single forward pass.

3.1 Likelihood formulation

We start by defining a joint dynamical system of states and beliefs (Van Den Berg et al., 2011) in which each depends only on the state and belief at the previous time step and the noises. For that, we insert the policy into the dynamics and the policy and observation function into the belief dynamics, yielding the equation

$$\begin{bmatrix} \mathbf{x}_{t+1} \\ \mathbf{b}_{t+1} \end{bmatrix} = \begin{bmatrix} f(\mathbf{x}_t, \pi_t(\mathbf{b}_t, \boldsymbol{\xi}_t), \mathbf{v}_t) \\ \beta_t(\mathbf{b}_t, \pi_t(\mathbf{b}_t, \boldsymbol{\xi}_t), h(\mathbf{x}_t, \mathbf{w}_t)) \end{bmatrix} \quad (2)$$

$$=: g(\mathbf{x}_t, \mathbf{b}_t, \mathbf{v}_t, \mathbf{w}_t, \boldsymbol{\xi}_t). \quad (3)$$

For given values of \mathbf{x}_t and \mathbf{b}_t , this equation defines the distribution $p(\mathbf{x}_{t+1}, \mathbf{b}_{t+1} | \mathbf{x}_t, \mathbf{b}_t)$, as $\mathbf{v}_t, \mathbf{w}_t, \boldsymbol{\xi}_t$ are independent of \mathbf{x}_{t+1} and \mathbf{b}_{t+1} . In Section 3.2 we will introduce an approximation via linearization, which leads to a closed-form expression for $p(\mathbf{x}_{t+1}, \mathbf{b}_{t+1} | \mathbf{x}_t, \mathbf{b}_t)$.

One can use this Markovian joint dynamical system to compute the likelihood factors for each time step (Schultheis et al., 2021). To this end, we first rewrite the individual likelihood terms $p(\mathbf{x}_{t+1} | \mathbf{x}_{1:t})$ of Equation (1) by marginalizing over the agent’s belief at each time step, i.e.,

$$p(\mathbf{x}_{t+1} | \mathbf{x}_{1:t}) = \int p(\mathbf{x}_{t+1}, \mathbf{b}_{t+1} | \mathbf{x}_{1:t}) d\mathbf{b}_{t+1}. \quad (4)$$

As the belief is an internal quantity of the agent and thus not observable to the researcher, we keep track of its distribution, $p(\mathbf{b}_t | \mathbf{x}_{1:t})$. For this, we rewrite

$$\begin{aligned} p(\mathbf{x}_{t+1}, \mathbf{b}_{t+1} | \mathbf{x}_{1:t}) &= \int p(\mathbf{x}_{t+1}, \mathbf{b}_{t+1}, \mathbf{b}_t | \mathbf{x}_{1:t}) d\mathbf{b}_t \\ &= \int p(\mathbf{x}_{t+1}, \mathbf{b}_{t+1} | \mathbf{x}_t, \mathbf{b}_t) p(\mathbf{b}_t | \mathbf{x}_{1:t}) d\mathbf{b}_t, \end{aligned} \quad (5)$$

where we have exploited the fact that the joint dynamical system of states and beliefs is Markovian. The distribution $p(\mathbf{b}_t | \mathbf{x}_{1:t})$ acts as a summary of the past states and can be computed by conditioning on the current state, i.e.,

$$p(\mathbf{b}_t | \mathbf{x}_{1:t}) = \frac{p(\mathbf{x}_t, \mathbf{b}_t | \mathbf{x}_{1:t-1})}{p(\mathbf{x}_t | \mathbf{x}_{1:t-1})}. \quad (6)$$

After determining $p(\mathbf{b}_t | \mathbf{x}_{1:t})$, we can propagate it through the joint dynamical system to arrive at the distribution $p(\mathbf{x}_{t+1}, \mathbf{b}_{t+1} | \mathbf{x}_{1:t})$. To obtain the belief distribution of the following time step, $p(\mathbf{b}_{t+1} | \mathbf{x}_{1:t+1})$, we condition on the observed state \mathbf{x}_{t+1} . To obtain the likelihood contribution, on the other hand, we marginalize out the \mathbf{b}_{t+1} .

To summarize, starting with an initialization $p(\mathbf{b}_0)$, we can compute the individual terms $p(\mathbf{x}_{t+1} | \mathbf{x}_{1:t})$ of the likelihood by executing Algorithm 1.

Algorithm 1 Approximate likelihood computation

Output: Approximate likelihood of parameters $p(\mathbf{x}_{1:T} | \boldsymbol{\theta})$

Input: Parameters $\boldsymbol{\theta}$, Data $\mathbf{x}_{1:T}$, Model f, h

- 1: Determine the policy π using iLQG
 - 2: Determine the belief dynamics β using the EKF
 - 3: **for** t in $\{1, \dots, T-1\}$ **do**
 - 4: Compute $p(\mathbf{x}_{t+1}, \mathbf{b}_{t+1} | \mathbf{x}_{1:t})$ using Equation (5)
 - 5: Update $p(\mathbf{b}_{t+1} | \mathbf{x}_{1:t+1})$ using Equation (6)
 - 6: Obtain $p(\mathbf{x}_{t+1} | \mathbf{x}_{1:t})$ using Equation (4)
 - 7: **end for**
-

3.2 Tractable likelihood via linearization

While the marginalization and propagating operations listed in the previous section can be done in closed form for linear-Gaussian systems, this is no longer feasible for non-linear systems. Therefore, we follow the approach of local linearization used in iLQG (Section 2.2) and the extended Kalman filter (Section 2.4). For the belief statistics, we consider the mean of the agent’s belief, i.e., $\mathbf{b}_t = \mathbb{E}[\mathbf{x}_t | \mathbf{y}_1, \dots, \mathbf{y}_{t-1}]$ and initialize the distribution for the first time step as a Gaussian, $p(\mathbf{b}_1) = \mathcal{N}(\mu_1^{(b)}, \Sigma_1^{(b)})$. We then approximate the distribution $p(\mathbf{x}_{t+1}, \mathbf{b}_{t+1} | \mathbf{x}_t, \mathbf{b}_t)$ as a Gaussian by applying a first-order Taylor expansion of g .

In order to obtain a closed-form expression for g , which we can linearize, we model the agent’s belief dynamics using the extended Kalman filter (Section 2.4) and its policy using iLQG (Section 2.2), as in the partially observable version of iLQG (Li and Todorov, 2007). This choice leads to an affine control law and belief dynamics given \mathbf{b}_t , making linearization of $p(\mathbf{x}_{t+1}, \mathbf{b}_{t+1} | \mathbf{x}_t, \mathbf{b}_t)$ straight-forward. To allow for additional stochasticity in the agent’s policy, we follow the common formulation of maximum causal entropy (MCE) reinforcement learning (Section 2.3). For the linearized dynamics, the MCE policy is – as for the fully-observable case (Section 2.3) – given by a Gaussian distribution, so that $\pi_t(\mathbf{b}_t, \boldsymbol{\xi}_t) = L_t(\mathbf{b}_t - \bar{\mathbf{x}}_{1:T}) + \mathbf{m}_t + \bar{\mathbf{u}}_{1:T} - \tilde{L}_t \boldsymbol{\xi}_t$, with \tilde{L}_t the Cholesky decomposition of L_t , and can be marginalized out in closed form.

The approximations we have introduced allow us to solve the integral in Equation (5) in closed form by applying standard equations for linear transformations of Gaussians, resulting in

$$p(\mathbf{x}_{t+1}, \mathbf{b}_{t+1} | \mathbf{x}_{1:t}) \approx \mathcal{N}(\mu_t, \Sigma_t) \quad (7)$$

with

$$\begin{aligned} \mu_t &= g(\mathbf{x}_t, \mu_t^{(b)}, 0, 0, 0), \\ \Sigma_t &= J_{\mathbf{b}} \Sigma_t^{(b)} J_{\mathbf{b}}^T + J_{\mathbf{v}} J_{\mathbf{v}}^T + J_{\mathbf{w}} J_{\mathbf{w}}^T + J_{\boldsymbol{\xi}} J_{\boldsymbol{\xi}}^T, \end{aligned}$$

where J_{\bullet} denotes the Jacobian of g w.r.t. \bullet , evaluated at $(\mathbf{x}_t, \mu_t^{(b)}, 0, 0, 0)$. Under this Gaussian approximation, both remaining operations of Algorithm 1 can also be performed in closed form. A more detailed derivation and representation of these formulas can be found in Appendix B. If the agent has full observations of the system’s state, the inverse optimal control problem is simplified significantly. The derivations for this special case are shown in Appendix C. Details about the implementation are provided in Appendix D.

3.3 Data-based linearization

The described approach to evaluate the likelihood requires solving the optimal filtering and control problem for a given set of parameters. When iteratively maximizing the likelihood, we would have to solve both problems in every iteration, making the approach computationally expensive. We can make the method more efficient by using the insight that in the IOC problem, we are given a trajectory $\mathbf{x}_{1:T}$. Instead of starting with a randomly initialized nominal trajectory and iterating between computation of the locally optimal control law and linearizing again, we can simply linearize the dynamics once around the given trajectory and keep this linearization fixed. We then need to perform only one backward-pass to compute an approximately optimal control law given the current parameters, and a forward pass to compute an approximately optimal filter. This, in particular, allows efficient computation of the gradient of the likelihood function. As we assume the actions to be unobservable, but they are needed for the linearization, we compute estimates of the actions by minimizing the squared difference of the noiseless state estimates and the actual states. Note that these estimated actions are only used for the linearization, but are not used as observed actions in the IOC likelihood itself (see Appendix E).

4 Experiments

We evaluated our proposed method on simulated data of two classic control tasks (Pendulum and CartPole) and two behavioral human tasks (reaching and navigation). To evaluate the accuracy of the parameter estimates obtained by our method and to compare it against a baseline, we computed absolute relative errors per parameter $|(\theta - \hat{\theta})/\theta|$. This makes averages across parameters on different scales more interpretable compared to other metrics like root mean squared errors. For each task, we simulated 100 sets of parameters from a uniform distribution in logarithmic space. For each set of parameters, we simulated 50 trajectories. We then maximized the log likelihood using gradient-based optimization with automatic differentiation (L-BFGS algorithm; Zhu et al., 1997). See Appendix G for a summary of the hyperparameters of our experiments.

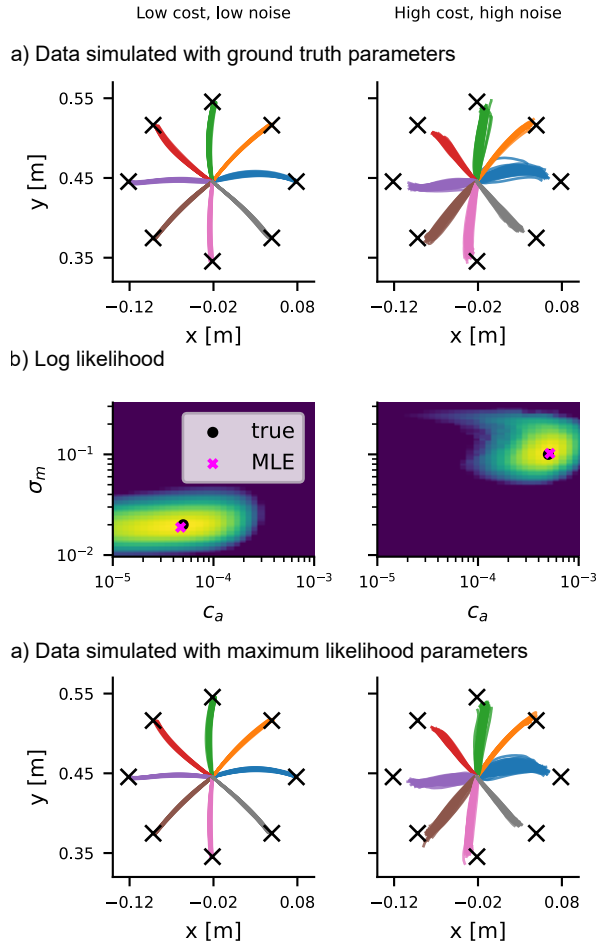


Figure 2: **IOC likelihood for the non-linear reaching task.** (a) Simulated reaching trajectories for eight targets. Increasing the cost of actions and the motor noise has an effect on the trajectories, since perfectly reaching the target becomes less important to the agent and variability increases. (b) IOC log likelihood for two of the model parameters, action costs c_a and motor noise σ_m . The likelihood has its maximum (pink cross) close to the ground truth parameter values (black dot). (c) Simulated trajectories using the MLEs from (b). The simulations are visually indistinguishable from the ground truth data.

All tasks we consider have four free parameters: cost of actions c_a , cost of velocity at the final time step c_v , motor noise σ_m , and observation noise σ_o . In the fully observable case, we leave out the observation noise parameter and only infer the three remaining parameters. For concrete definitions of the parameters in each specific tasks, see Appendix F.

4.1 Baseline method

For a comparison to previously proposed methods, we applied a baseline method based on the maximum causal entropy (MCE) approach (Ziebart et al., 2010), as these formulations have been successfully used for IOC in non-linear stochastic systems. As to the best of our knowledge, no past method can be directly applied in the setting we consider (non-linear and stochastic dynamics, unknown controls, partial observability, finite horizon), we choose a straight-forward implementation of the MCE formulation for this case. The tasks we consider can be well solved by linearizing the dynamics locally, so an accurate approximation of the optimal MCE controller is given by the optimal MCE controller for the linearized dynamics (see Section 2.3). An estimate of the parameters is then obtained by maximizing the likelihood of the approximate maximum entropy policy for the given set of states and controls. To apply this baseline to the setting where control signals are missing, we use the estimates of the controls as we determine in our proposed method for the data-based linearization (Section 3.3). As past IOC methods do not have an explicit model of partial observability, except for a few exceptions which are limited to specific tasks, we follow the usual formulation of the policy acting directly on the states. To show that this approach constitutes a suitable baseline, in Appendix H.3, we provide results for the case where the true control signals are known and there is no partial observability.

4.2 Reaching task

We evaluate the method on a manual reaching task with a non-linear biomechanical model of a two-link arm. The agent’s goal is to move its arm towards a target in the horizontal plane by controlling its two joints. For a more detailed description, see Appendix F.2. Note that the cost function is non-linear in states because the positions are a non-linear function of the joint angles that comprise the state of the system. We use a fully observable version of the task (Todorov and Li, 2005) and a version in which the agent receives noisy observations (Li and Todorov, 2007). This model has been applied to reaching movements in the sensorimotor neuroscience literature (e.g., Nagengast et al., 2009; Knill et al., 2011). Figure 2a shows simulations from the model using iLQG with two different parameter settings. We evaluated the likelihood function for a grid of two of the model parameters (Figure 2b) to illustrate that it has well-defined maxima close to the true parameter values. In this example, simulated data using the maximum likelihood estimates look indistinguishable from the ground truth data (Figure 2c).

In Figure 3 we present maximum likelihood parameter estimates and true values for repeated runs with different random parameter settings. One can observe that the parameter estimates of our method closely align with the true parameter values, showing that our method can successfully recover the parameters from data. The baseline method, in contrast, shows considerably worse performance, in particular for estimating noises. Estimates for the fully observable case are provided in Appendix H.2. To quantify the accuracy of the maximum likelihood estimates, we computed the absolute relative errors. The results are shown separately for the fully observable and partially observable cases in Figure 4. The median absolute relative errors of our method were 0.11, while they were 0.93 for the baseline. The influence of missing control signals and of the lacking explicit observation model in the baseline can be observed by comparing the results to the fully-observable case and the case of given control signals in Appendix H.2 and Appendix H.3.

4.3 Navigation task

In the navigation task, we consider an agent navigating to a target under non-linear dynamics while receiving noisy observations from a non-linear observation model. To reach the target, the agent can control the angular velocity of their heading direction and the acceleration with which they move forward. The agent observes noisy versions of the distance to the target and the target’s bearing angle. We provide more details about the experiment in Appendix F.3.

Maximum likelihood parameter estimates for the navigation task are shown for the partially observable case in Figure S4 and for the fully observable case in Figure S8. As for the reaching task, our method provides parameter estimates close to the true ones, while the estimates of the baseline deviate for a large number of trials. Median absolute relative errors of our method were 0.31, while they were 1.99 for the baseline (Figure 4).

4.4 Classic control tasks

Lastly, we evaluate our method on two classic control tasks (Pendulum and Cart Pole) based on the implementations in the gym library (Brockman et al., 2016). Because these tasks are neither stochastic nor partially observable in their standard formulations, we introduce noise on the dynamics and turn them into partially-observed problems by defining a stochastic observation function (see Appendix F.1). In Appendix H we show the parameter estimates for the Pendulum (Figure S2) and for the Cart Pole (Figure S3) for the partially ob-

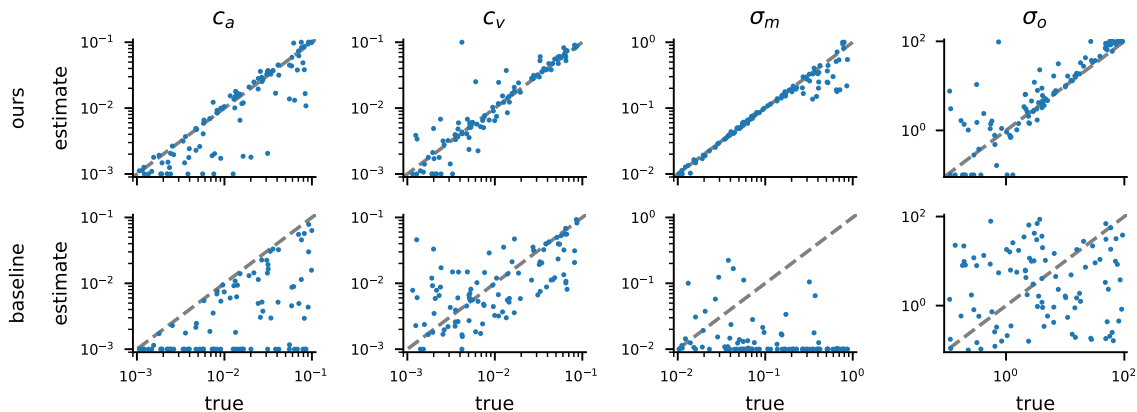


Figure 3: **Maximum likelihood estimates for reaching task** True parameter values plotted against the maximum likelihood parameter estimates for the partially observable reaching task. Top row: our method, bottom row: MCE baseline. The columns contain the four different model parameters (action cost c_a , velocity cost c_v , motor noise σ_m , observation noise σ_o).

servable case, while Figure S6 and Figure S7 show the fully observable case, respectively. One can observe that the results match the ones of the reaching and navigation task, showing that our method provides accurate estimates of the parameters. Median absolute relative errors of our method were 0.12 and 0.41, while for the baseline they were 2.21 and 3.82 (Figure 4).

5 Conclusion

In this paper, we introduced a new method for inverse optimal control for systems with stochastic dynamics, partial observability, and missing control signals. We followed a probabilistic formulation of the problem, where the goal is formulated as maximizing the likelihood of the observed states given the parameters. As the exact evaluation of the likelihood for a general non-linear model is intractable, we developed an efficient approximation of the likelihood by linearizing the system locally around the given trajectories, as in popular approaches such as the extended Kalman filter or iLQG. By maintaining a Gaussian distribution that tracks the agent’s state estimate, the proposed method is able to evaluate an approximate likelihood in closed form within a single forward pass.

Besides offering an efficient way to evaluate the likelihood, our proposed formulation is able to incorporate multiple sources of the stochasticity of the agent through an explicit model of the partial observability and by modelling control via a maximum causal entropy (MCE) policy. Our method thereby reconciles the theory of past MCE IOC algorithms (e.g., Ziebart et al., 2010) and approaches where the agent’s stochasticity stems from an explicit stochastic observation model

(Schultheis et al., 2021).

We have applied our method to two stochastic variations of classical control tasks, the pendulum and cart pole, and to two human behavioral tasks, a reaching and navigation tasks. In the comparison to a MCE baseline, for which missing control signals need to be estimated, we have found our method to achieve lower estimation errors across all evaluated tasks. Further, it successfully inferred noise parameters of the system, which was not possible with the baseline.

The limitations of our method are mainly due to the linearization of the dynamical system and the Gaussian approximations involved in the belief tracking formulation of the likelihood function. In more complex scenarios with belief distributions that are not well approximated by a Gaussian, e.g., multimodal beliefs, the method is likely to produce inaccurate results. This problem could be addressed by replacing the closed-form Gaussian approximation of the belief by particle-based methods (Doucet et al., 2001). Further, we focused on tasks which could be solved well by applying controllers based on linearization and Gaussian approximation (iLQG and EKF), motivated by their popularity in applications in cognitive science and neuroscience. High-dimensional problems that cannot be solved forward using iLQG, in contrast, are probably not directly solvable using our proposed method. While, in principle, our method is also applicable using other forward control methods that compute differentiable policies, it is unclear whether linearizing these policies leads to accurate approximate likelihoods and parameter estimates.

A further limitation of our method is that it requires parametric models of the dynamics and noise structure.

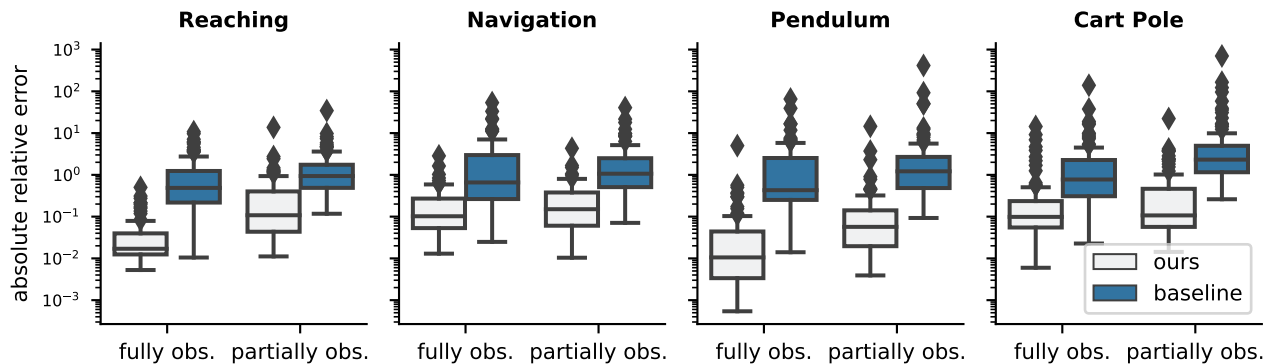


Figure 4: **Evaluation across tasks.** Absolute relative errors (log scale) for different tasks. Our method consistently outperforms the MCE baseline.

While single missing parameters can be determined using our method, in the case of completely unknown dynamics a model-free approach to IOC would be more suitable.

Lastly, while we have shown that inference of few parameters is feasible, the results probably do not scale to a large number of parameters. One reason for this is that optimization in a high-dimensional non-linear space becomes difficult, and one can potentially get stuck in local minima. This problem could be relieved by using more advanced optimization methods. A further, more fundamental, concern with a large number of parameters is that parameters are likely to become not unambiguously identifiable and there is no unique solution. However, in many scientific fields, knowledge about the structure and parametric models describing the agent’s uncertainty and internal model are available or measurable, allowing our method to be used successfully. Moreover, our probabilistic approach with a closed-form likelihood opens up the possibility of using Bayesian methods to investigate the identifiability of model parameters (Acerbi et al., 2014).

Our proposed method provides a tool for researchers interested in modeling sequential behavior, e.g., in sensorimotor domains, allowing to infer an agent’s subjective costs and internal uncertainties. This will enable answering novel scientific questions about how these quantities are affected by different experimental conditions, deviate from intended task goals and provided task instructions, or how they vary between individuals. This is particularly relevant to a computational understanding of naturalistic behavior (Krakauer et al., 2017; Cisek and Pastor-Bernier, 2014; Miller et al., 2022), for which subjective utilities are mostly unknown.

Acknowledgements

The authors gratefully acknowledge the computing time provided to them on the high-performance computer Lichtenberg at the NHR Centers NHR4CES at TU Darmstadt, and financial support by the project “Whitebox” funded by the Priority Program LOEWE of the Hessian Ministry of Higher Education, Science, Research and Art.

References

- Abbeel, P. and Ng, A. Y. (2004). Apprenticeship learning via inverse reinforcement learning. In *International Conference on Machine Learning*, volume 5.
- Acerbi, L., Ma, W. J., and Vijayakumar, S. (2014). A framework for testing identifiability of bayesian models of perception. In *Advances in Neural Information Processing Systems*, volume 27.
- Aghasadeghi, N. and Bretl, T. (2011). Maximum entropy inverse reinforcement learning in continuous state spaces with path integrals. In *International Conference on Intelligent Robots and Systems*, pages 1561–1566.
- Anderson, B. D. and Moore, J. B. (1990). Optimal control: linear quadratic methods.
- Ashwood, Z., Roy, N. A., Bak, J. H., and Pillow, J. W. (2020). Inferring learning rules from animal decision-making. In *Advances in Neural Information Processing Systems*, volume 33, pages 3442–3453.
- Åström, K. J. (1965). Optimal control of markov processes with incomplete state information i. *Journal of Mathematical Analysis and Applications*, 10:174–205.

- Bishop, C. M. and Nasrabadi, N. M. (2006). *Pattern recognition and machine learning*, volume 4. Springer.
- Blondel, M., Berthet, Q., Cuturi, M., Frostig, R., Hoyer, S., Llinares-López, F., Pedregosa, F., and Vert, J.-P. (2021). Efficient and modular implicit differentiation. *arXiv preprint arXiv:2105.15183*.
- Bogert, K., Lin, J. F.-S., Doshi, P., and Kulic, D. (2016). Expectation-maximization for inverse reinforcement learning with hidden data. In *International Conference on Autonomous Agents & Multiagent Systems*, pages 1034–1042.
- Boularias, A., Kober, J., and Peters, J. (2011). Relative entropy inverse reinforcement learning. In *International Conference on Artificial Intelligence and Statistics*, pages 182–189.
- Bradbury, J., Frostig, R., Hawkins, P., Johnson, M. J., Leary, C., Maclaurin, D., Necula, G., Paszke, A., VanderPlas, J., Wanderman-Milne, S., and Zhang, Q. (2018). JAX: composable transformations of Python+NumPy programs.
- Brockman, G., Cheung, V., Pettersson, L., Schneider, J., Schulman, J., Tang, J., and Zaremba, W. (2016). Openai gym. *arXiv preprint arXiv:1606.01540*.
- Chen, X. and Ziebart, B. (2015). Predictive inverse optimal control for linear-quadratic-Gaussian systems. In *Artificial Intelligence and Statistics*, pages 165–173.
- Choi, J. and Kim, K.-E. (2011). Inverse reinforcement learning in partially observable environments. *Journal of Machine Learning Research*, 12:691–730.
- Cisek, P. and Pastor-Bernier, A. (2014). On the challenges and mechanisms of embodied decisions. *Philosophical Transactions of the Royal Society B: Biological Sciences*, 369(1655):20130479.
- Doucet, A., De Freitas, N., Gordon, N. J., et al. (2001). *Sequential Monte Carlo methods in practice*, volume 1. Springer.
- Finn, C., Levine, S., and Abbeel, P. (2016). Guided cost learning: Deep inverse optimal control via policy optimization. In *International Conference on Machine Learning*, pages 49–58. PMLR.
- Garg, D., Chakraborty, S., Cundy, C., Song, J., and Ermon, S. (2021). IQ-learn: Inverse soft-Q learning for imitation. *Advances in Neural Information Processing Systems*, 34:4028–4039.
- Gleave, A. and Toyer, S. (2022). A primer on maximum causal entropy inverse reinforcement learning. *arXiv preprint arXiv:2203.11409*.
- Golub, M., Chase, S., and Yu, B. (2013). Learning an internal dynamics model from control demonstration. In *International Conference on Machine Learning*, pages 606–614.
- Harris, C. M. and Wolpert, D. M. (1998). Signal-dependent noise determines motor planning. *Nature*, 394(6695):780–784.
- Kaelbling, L. P., Littman, M. L., and Cassandra, A. R. (1998). Planning and acting in partially observable stochastic domains. *Artificial intelligence*, 101(1-2):99–134.
- Kahneman, D. and Tversky, A. (1979). Prospect theory: An analysis of decision under risk. *Econometrica*, 47(2):263–292.
- Kalman, R. E. (1960). A New Approach to Linear Filtering and Prediction Problems. *Journal of Basic Engineering*, 82(1):35–45.
- Kalman, R. E. (1964). When Is a Linear Control System Optimal? *Journal of Basic Engineering*, 86(1):51–60.
- Kappen, H. J., Gómez, V., and Opper, M. (2012). Optimal control as a graphical model inference problem. *Machine learning*, 87(2):159–182.
- Kessler, F., Frankenstein, J., and Rothkopf, C. A. (2022). A dynamic bayesian actor model explains endpoint variability in homing tasks. *bioRxiv*.
- Kitani, K. M., Ziebart, B. D., Bagnell, J. A., and Hebert, M. (2012). Activity forecasting. In *European Conference on Computer Vision*, pages 201–214. Springer.
- Knill, D. C., Bondada, A., and Chhabra, M. (2011). Flexible, task-dependent use of sensory feedback to control hand movements. *Journal of Neuroscience*, 31(4):1219–1237.
- Kochenderfer, M. J., Wheeler, T. A., and Wray, K. H. (2022). *Algorithms for decision making*. MIT press.
- Körding, K. P. and Wolpert, D. M. (2004). The loss function of sensorimotor learning. *Proceedings of the National Academy of Sciences*, 101(26):9839–9842.
- Krakauer, J. W., Ghazanfar, A. A., Gomez-Marín, A., MacIver, M. A., and Poeppel, D. (2017). Neuroscience needs behavior: correcting a reductionist bias. *Neuron*, 93(3):480–490.

- Kwon, M., Daptardar, S., Schrater, P. R., and Pitkow, X. (2020). Inverse rational control with partially observable continuous nonlinear dynamics. *Advances in Neural Information Processing Systems*, 33:7898–7909.
- Levine, S. (2018). Reinforcement learning and control as probabilistic inference: Tutorial and review. *arXiv preprint arXiv:1805.00909*.
- Levine, S. and Koltun, V. (2012). Continuous inverse optimal control with locally optimal examples. In *International Conference on Machine Learning*, pages 475–482.
- Levine, S. and Koltun, V. (2013). Guided policy search. In *International Conference on Machine Learning*, pages 1–9.
- Li, W. (2006). *Optimal control for biological movement systems*. PhD thesis, UC San Diego.
- Li, W. and Todorov, E. (2007). Iterative linearization methods for approximately optimal control and estimation of non-linear stochastic system. *International Journal of Control*, 80(9):1439–1453.
- Li, W., Todorov, E., and Liu, D. (2011). Inverse optimality design for biological movement systems. *IFAC Proceedings Volumes*, 44(1):9662–9667.
- Miller, C. T., Gire, D., Hoke, K., Huk, A. C., Kelley, D., Leopold, D. A., Smear, M. C., Theunissen, F., Yartsev, M., and Niell, C. M. (2022). Natural behavior is the language of the brain. *Current Biology*, 32(10):R482–R493.
- Mombaur, K., Truong, A., and Laumond, J.-P. (2010). From human to humanoid locomotion – an inverse optimal control approach. *Autonomous Robots*, 28(3):369–383.
- Mosteller, F. and Nogee, P. (1951). An experimental measurement of utility. *Journal of Political Economy*, 59(5):371–404.
- Muelling, K., Boularias, A., Mohler, B., Schölkopf, B., and Peters, J. (2014). Learning strategies in table tennis using inverse reinforcement learning. *Biological Cybernetics*, 108(5):603–619.
- Nagengast, A. J., Braun, D. A., and Wolpert, D. M. (2009). Optimal control predicts human performance on objects with internal degrees of freedom. *PLoS Computational Biology*, 5(6):e1000419.
- Ng, A. Y., Russell, S. J., et al. (2000). Algorithms for inverse reinforcement learning. In *International Conference on Machine Learning*, volume 1.
- Osa, T., Pajarinen, J., Neumann, G., Bagnell, J. A., Abbeel, P., Peters, J., et al. (2018). An algorithmic perspective on imitation learning. *Foundations and Trends in Robotics*, 7(1-2):1–179.
- Rothkopf, C. A. and Ballard, D. H. (2013). Modular inverse reinforcement learning for visuomotor behavior. *Biological cybernetics*, 107(4):477–490.
- Rothkopf, C. A. and Dimitrakakis, C. (2011). Preference elicitation and inverse reinforcement learning. In *Machine Learning and Knowledge Discovery in Databases: European Conference, ECML PKDD 2011, Athens, Greece, September 5-9, 2011, Proceedings, Part III 22*, pages 34–48. Springer.
- Schmitt, F., Bieg, H.-J., Herman, M., and Rothkopf, C. A. (2017). I see what you see: Inferring sensor and policy models of human real-world motor behavior. In *AAAI Conference on Artificial Intelligence*.
- Schmitt, F., Bieg, H.-J., Manstetten, D., Herman, M., and Stiefelwagen, R. (2016). Exact maximum entropy inverse optimal control for modeling human attention switching and control. In *IEEE International Conference on Systems, Man, and Cybernetics*, pages 2807–2813.
- Schultheis, M., Rothkopf, C. A., and Koepl, H. (2022). Reinforcement learning with non-exponential discounting. In *Advances in Neural Information Processing Systems*, volume 35.
- Schultheis, M., Straub, D., and Rothkopf, C. A. (2021). Inverse optimal control adapted to the noise characteristics of the human sensorimotor system. *Advances in Neural Information Processing Systems*, 34.
- Silva, J. A., Grassi, V., and Wolf, D. F. (2019). Continuous deep maximum entropy inverse reinforcement learning using online POMDP. In *IEEE International Conference on Advanced Robotics*, volume 19, pages 382–387.
- Straub, D. and Rothkopf, C. A. (2022). Putting perception into action with inverse optimal control for continuous psychophysics. *Elife*, 11:e76635.
- Taylor, M. E. and Stone, P. (2009). Transfer learning for reinforcement learning domains: A survey. *Journal of Machine Learning Research*, 10(7).
- Todorov, E. and Jordan, M. I. (2002). Optimal feedback control as a theory of motor coordination. *Nature neuroscience*, 5(11):1226–1235.
- Todorov, E. and Li, W. (2005). A generalized iterative LQG method for locally-optimal feedback control of

- constrained nonlinear stochastic systems. In *American Control Conference*, pages 300–306. IEEE.
- Toussaint, M. (2009). Robot trajectory optimization using approximate inference. In *International Conference on Machine Learning*, pages 1049–1056.
- Van Den Berg, J., Abbeel, P., and Goldberg, K. (2011). LQG-MP: Optimized path planning for robots with motion uncertainty and imperfect state information. *The International Journal of Robotics Research*, 30(7):895–913.
- Virtanen, P., Gommers, R., Oliphant, T. E., Haberland, M., Reddy, T., Cournapeau, D., Burovski, E., Peterson, P., Weckesser, W., Bright, J., et al. (2020). Scipy 1.0: fundamental algorithms for scientific computing in python. *Nature methods*, 17(3):261–272.
- Wolpert, D. M. and Ghahramani, Z. (2000). Computational principles of movement neuroscience. *Nature neuroscience*, 3(11):1212–1217.
- Zhu, C., Byrd, R. H., Lu, P., and Nocedal, J. (1997). Algorithm 778: L-BFGS-B: Fortran subroutines for large-scale bound-constrained optimization. *ACM Transactions on Mathematical Software (TOMS)*, 23(4):550–560.
- Ziebart, B. D., Bagnell, J. A., and Dey, A. K. (2010). Modeling interaction via the principle of maximum causal entropy. In *International Conference on Machine Learning*.
- Ziebart, B. D., Maas, A. L., Bagnell, J. A., Dey, A. K., et al. (2008). Maximum entropy inverse reinforcement learning. In *AAAI*, volume 23, pages 1433–1438.

Appendix

A Notation

Table 1: Notation

$\mathbf{x}_t \in \mathbb{R}^n$	state at time t
$\mathbf{u}_t \in \mathbb{R}^u$	action at time t
$\mathbf{y}_t \in \mathbb{R}^m$	observation at time t
$T \in \mathbb{N}$	number of time steps
$f : \mathbb{R}^n \times \mathbb{R}^u \times \mathbb{R}^v \rightarrow \mathbb{R}^n$	system dynamics function
$h : \mathbb{R}^n \times \mathbb{R}^w \rightarrow \mathbb{R}^m$	observation function
$\mathbf{v}_t \in \mathbb{R}^v$	standard multivariate normal dynamics noise
$\mathbf{w}_t \in \mathbb{R}^w$	standard multivariate normal observation noise
$c_t : \mathbb{R}^n \times \mathbb{R}^u \rightarrow \mathbb{R}$	cost function at intermediate time steps
$c_T : \mathbb{R}^n \rightarrow \mathbb{R}$	cost function at final time step
$\mathbf{b}_t \in \mathbb{R}^b$	summary statistics of agent's belief, $p(\mathbf{x}_t \mathbf{y}_{1:t-1})$
$\beta_t : \mathbb{R}^b \times \mathbb{R}^u \times \mathbb{R}^m \rightarrow \mathbb{R}^b$	belief dynamics
$\pi_t : \mathbb{R}^b \times \mathbb{R}^j \rightarrow \mathbb{R}^u$	policy of the agent
$\boldsymbol{\theta} \in \mathbb{R}^p$	model parameters
$g : \mathbb{R}^n \times \mathbb{R}^b \times \mathbb{R}^v \times \mathbb{R}^w \times \mathbb{R}^j \rightarrow \mathbb{R}^n \times \mathbb{R}^b$	joint dynamics of states and beliefs

B Inverse optimal control derivations

We start with defining the joint dynamics of states and estimates, which returns the next state and estimate as a function of the previous state and estimate and the noises,

$$\begin{bmatrix} \mathbf{x}_{t+1} \\ \mathbf{b}_{t+1} \end{bmatrix} = g(\mathbf{x}_t, \mathbf{b}_t, \mathbf{v}_t, \mathbf{w}_t, \boldsymbol{\xi}_t). \quad (8)$$

To do so, we insert the policy and observation function into the system and belief dynamics, giving

$$\mathbf{x}_{t+1} = f(\mathbf{x}_t, \pi_t(\mathbf{b}_t, \boldsymbol{\xi}_t), \mathbf{v}_t), \quad (9)$$

$$\mathbf{b}_{t+1} = \beta_t(\mathbf{b}_t, \pi_t(\mathbf{b}_t, \boldsymbol{\xi}_t), h(\mathbf{x}_t, \mathbf{w}_t)). \quad (10)$$

The individual factors of the likelihood function can be determined as

$$p(\mathbf{x}_{t+1} | \mathbf{x}_{1:t}) = \int p(\mathbf{x}_{t+1}, \mathbf{b}_{t+1} | \mathbf{x}_{1:t}) d\mathbf{b}_{t+1},$$

where $p(\mathbf{x}_{t+1}, \mathbf{b}_{t+1} | \mathbf{x}_{1:t})$ is given by marginalizing over the current belief \mathbf{b}_t as

$$\begin{aligned} p(\mathbf{x}_{t+1}, \mathbf{b}_{t+1} | \mathbf{x}_{1:t}) &= \int p(\mathbf{x}_{t+1}, \mathbf{b}_{t+1}, \mathbf{b}_t | \mathbf{x}_{1:t}) d\mathbf{b}_t \\ &= \int p(\mathbf{x}_{t+1}, \mathbf{b}_{t+1} | \mathbf{x}_{1:t}, \mathbf{b}_t) p(\mathbf{b}_t | \mathbf{x}_{1:t}) d\mathbf{b}_t \\ &= \int p(\mathbf{x}_{t+1}, \mathbf{b}_{t+1} | \mathbf{x}_t, \mathbf{b}_t) p(\mathbf{b}_t | \mathbf{x}_{1:t}) d\mathbf{b}_t. \end{aligned}$$

Linearization

To derive a tractable approximation of the distribution $p(\mathbf{x}_{t+1}, \mathbf{b}_{t+1} | \mathbf{x}_{1:t})$, we model the initial belief of the agent's state estimate $p(\mathbf{b}_1)$ as a Gaussian and linearize the joint dynamics function, leading to a Gaussian approximation of the desired quantity, i.e., $p(\mathbf{x}_{t+1}, \mathbf{b}_{t+1} | \mathbf{x}_{1:t}) \approx \mathcal{N}(\boldsymbol{\mu}_t, \boldsymbol{\Sigma}_t)$.

First, we apply a first-order Taylor expansion of the joint dynamics g around the observed state \mathbf{x}_t and the mean of the belief $\mu_t^{(b)}$ and the noises:

$$g(\mathbf{x}_t, \mathbf{b}_t, \mathbf{v}_t, \mathbf{w}_t, \boldsymbol{\xi}_t) \approx g(\mathbf{x}_t, \mu_t^{(b)}, 0, 0, 0) + J_{\mathbf{b}}(\mathbf{b}_t - \mu_t^{(b)}) + J_{\mathbf{v}}\mathbf{v}_t + J_{\mathbf{w}}\mathbf{w}_t + J_{\boldsymbol{\xi}}\boldsymbol{\xi}_t, \quad (11)$$

where J_{\bullet} denotes the Jacobian of g w.r.t. \bullet , evaluated at $(\mathbf{x}_t, \mu_t^{(b)}, 0, 0, 0)$.

To derive an explicit representation of the Jacobians, we insert the filtering and control law obtained by the Kalman filter and maximum entropy iLQG controller and find

$$\begin{aligned} g(\mathbf{x}_t, \mathbf{b}_t, \mathbf{v}_t, \mathbf{w}_t, \boldsymbol{\xi}_t) &= \begin{bmatrix} f(\mathbf{x}_t, \pi_t(\mathbf{b}_t, \boldsymbol{\xi}_t), \mathbf{v}_t) \\ \beta_t(\mathbf{b}_t, \pi_t(\mathbf{b}_t, \boldsymbol{\xi}_t), h(\mathbf{x}_t, \mathbf{w}_t)) \end{bmatrix} \\ &= \begin{bmatrix} f(\mathbf{x}_t, \mathbf{u}_t, \mathbf{v}_t) \\ \beta_t(\mathbf{b}_t, \mathbf{u}_t, \mathbf{y}_t) \end{bmatrix}, \end{aligned}$$

with

$$\begin{aligned} \mathbf{y}_t &= h(\mathbf{x}_t, \mathbf{w}_t), \\ \mathbf{u}_t &= \pi_t(\mathbf{b}_t, \boldsymbol{\xi}_t) = L_t(\mathbf{b}_t - \bar{\mathbf{x}}_{1:T}) + \mathbf{m}_t + \bar{\mathbf{u}}_{1:T} - \tilde{L}_t\boldsymbol{\xi}_t, \\ \beta_t(\mathbf{b}_t, \mathbf{u}_t, \mathbf{y}_t) &= f(\mathbf{b}_t, \mathbf{u}_t, 0) + K_t(\mathbf{y}_t - h(\mathbf{b}_t, 0)), \end{aligned}$$

leading to the equations

$$\begin{aligned} J_{\mathbf{b}} &= \begin{bmatrix} \nabla_{\mathbf{u}}f(\mathbf{x}_t, \mathbf{u}_t, 0)\nabla_{\mathbf{b}}\mathbf{u}_t \\ \nabla_{\mathbf{b}}\beta_t(\mathbf{b}_t, \mathbf{u}_t, \mathbf{y}_t) + \nabla_{\mathbf{u}}\beta_t(\mathbf{b}_t, \mathbf{u}_t, \mathbf{y}_t)\nabla_{\mathbf{b}}\mathbf{u}_t \end{bmatrix} \\ &= \begin{bmatrix} \nabla_{\mathbf{u}}f(\mathbf{x}_t, \mathbf{u}_t, 0)L_t \\ \nabla_{\mathbf{x}}f(\mathbf{b}_t, \mathbf{u}_t, 0) - K_t\nabla_{\mathbf{x}}h(\mathbf{b}_t, 0) + \nabla_{\mathbf{u}}f(\mathbf{b}_t, \mathbf{u}_t, 0)L_t \end{bmatrix}, \\ J_{\mathbf{v}} &= \begin{bmatrix} \nabla_{\mathbf{v}}f(\mathbf{x}_t, \mathbf{u}_t, 0) \\ \nabla_{\mathbf{v}}f(\mathbf{b}_t, \mathbf{u}_t, 0) \end{bmatrix}, \\ J_{\mathbf{w}} &= \begin{bmatrix} 0 \\ \nabla_{\mathbf{h}}\beta_t(\mathbf{b}_t, \mathbf{u}_t, \mathbf{y}_t)\nabla_{\mathbf{w}}h(\mathbf{b}_t, 0) \end{bmatrix} = \begin{bmatrix} 0 \\ -K_t\nabla_{\mathbf{w}}h(\mathbf{b}_t, 0) \end{bmatrix}, \\ J_{\boldsymbol{\xi}} &= \begin{bmatrix} \nabla_{\mathbf{u}}f(\mathbf{x}_t, \mathbf{u}_t, 0)\nabla_{\boldsymbol{\xi}}\mathbf{u}_t \\ \nabla_{\mathbf{u}}f(\mathbf{b}_t, \mathbf{u}_t, 0)\nabla_{\boldsymbol{\xi}}\mathbf{u}_t \end{bmatrix} = \begin{bmatrix} \nabla_{\mathbf{u}}f(\mathbf{x}_t, \mathbf{u}_t, 0)L_t \\ \nabla_{\mathbf{u}}f(\mathbf{b}_t, \mathbf{u}_t, 0)L_t \end{bmatrix}. \end{aligned}$$

Propagating the Gaussian belief over the agent's state estimate, $p(\mathbf{b}_t | \mathbf{x}_{1:t})$ through the linearized dynamics model (Equation (5)) can be done by applying standard identities for linear transformations of Gaussian random variables (Bishop and Nasrabadi, 2006) and gives

$$p(\mathbf{x}_{t+1}, \mathbf{b}_{t+1} | \mathbf{x}_{1:t}) \approx \mathcal{N}(\mu_t, \Sigma_t), \quad (12)$$

with $\mu_t = g(\mathbf{x}_t, \mu_t^{(b)}, 0, 0, 0)$ and $\Sigma_t = J_{\mathbf{b}}\Sigma_t^{(b)}J_{\mathbf{b}}^T + J_{\mathbf{v}}J_{\mathbf{v}}^T + J_{\mathbf{w}}J_{\mathbf{w}}^T + J_{\boldsymbol{\xi}}J_{\boldsymbol{\xi}}^T$. Marginalization over \mathbf{b}_{t+1} gives the desired likelihood factor, while conditioning on \mathbf{x}_{t+1} gives the belief statistic for the following time step (see Section 3.1).

C Special case: full observability

If the state \mathbf{x}_t is fully observable to the agent, the problem is simplified significantly. The control problem from the agent’s perspective (Figure S1, left) can be solved by applying iLQG (Todorov and Li, 2005) to the observed states directly (Section 2.2)

$$\mathbf{u}_t = \pi_t(\mathbf{x}_t, \boldsymbol{\xi}_t), \quad (13)$$

This also simplifies the IOC problem from the researcher’s perspective because evaluating the approximate likelihood becomes straight-forward as we do not need to marginalize over the agent’s belief.

Recall that the likelihood can be decomposed as

$$p(\mathbf{x}_{1:T} | \theta) = p(\mathbf{x}_0 | \theta) \prod_{t=0}^{T-1} p(\mathbf{x}_{t+1} | \mathbf{x}_{1:t}, \theta) \quad (14)$$

and the dynamics are given as

$$\mathbf{x}_{t+1} = f(\mathbf{x}_t, \mathbf{u}_t, \mathbf{v}_t) = f(\mathbf{x}_t, \pi(\mathbf{x}_t, \boldsymbol{\xi}_t), \mathbf{v}_t). \quad (15)$$

We can approximate the likelihood contribution at each time step as

$$p(\mathbf{x}_{t+1} | \mathbf{x}_{1:t}, \theta) \approx \mathcal{N}(\mu_t, \Sigma_t), \quad (16)$$

with

$$\mu_t = f(\mathbf{x}_t, \pi(\mathbf{x}_t, 0), 0) \quad (17)$$

$$\Sigma_t = J_v J_v^T + J_\xi J_\xi^T, \quad (18)$$

where J_\bullet denotes the Jacobian of f w.r.t. \bullet , evaluated at $(\mathbf{x}_t, \pi(\mathbf{x}_t, 0), 0)$:

$$J_v = \nabla_v f(\mathbf{x}_t, \mathbf{u}_t, 0),$$

$$J_\xi = \nabla_u f(\mathbf{x}_t, \mathbf{u}_t, 0) \nabla_\xi \mathbf{u}_t = \nabla_u f(\mathbf{x}_t, \mathbf{u}_t, 0) L_t.$$

D Implementation

We provide a flexible framework for defining non-linear stochastic dynamical systems of the form introduced in Section 2.1 by implementing the dynamics, observation function, and cost function. The optimal estimation control methods based on iterative linearization are implemented using the automatic differentiation library `jax` (Bradbury et al., 2018), so that Jacobians and Hessians for the linearization of the dynamics and quadratization of the cost do not have to be specified manually. Furthermore, the Jacobians needed for linear-Gaussian approximation in the IOC likelihood (Section 3.2) are also computed using automatic differentiation. Gradient-based maximization of the log likelihood was performed using the L-BFGS-B `scipy` (Virtanen et al., 2020) from the `jaxopt` library (Blondel et al., 2021). The implementation will be made public upon publication.

For computations, we used an Intel Xeon Platinum 9242 Processor, using 1 core per run. The mean run times for computing maximum likelihood estimates (partially observable setting) were as follows:

- Reaching: 140 s
- Navigation: 64 s
- Pendulum: 31 s
- CartPole: 115 s

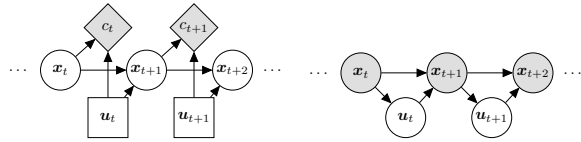


Figure S1: **Left:** decision network from the agent’s perspective (following the notation used in Kochenderfer et al., 2022). The agent directly observes the state \mathbf{x}_t . At each time step, they perform an action \mathbf{u}_t and incur a cost c_t . **Right:** probabilistic graphical model from the researcher’s perspective, who observes a trajectory $\mathbf{x}_{1:T}$ from an agent. The action signals \mathbf{u}_t are not directly observed.

E Estimating actions for linearization

For every evaluation of the likelihood function as described in Section 3.1, we would naively need to solve the forward control problem once by running the iLQG algorithm given the current parameter values. This is computationally inefficient due to the iterative procedure of iLQG, which requires multiple forward and backward passes. Instead of performing the iterative procedure, which computes the locally optimal control law $\{L_{1:T-1}, \mathbf{m}_{1:T-1}\}$ around a nominal trajectory $\{\bar{\mathbf{x}}_{1:T}, \bar{\mathbf{u}}_{1:T-1}\}$, then computes the new nominal trajectory given the current control law and so on, we realize that in the IOC setting, we already have observed the actual trajectory $\mathbf{x}_{1:T}$ performed by the agent. To make solving the forward control problem more efficient, we only compute the locally optimal control law once around this trajectory. This would require the action signals $\mathbf{u}_{1:T}$ to be given, but they are unobserved in our problem setting. To obtain a proxy for the actions for the purposes of linearization, we solve for the actions given the trajectory $\mathbf{x}_{1:T}$ in the system dynamics equation $\mathbf{x}_{t+1} = f(\mathbf{x}_t, \mathbf{u}_t, \mathbf{v}_t)$ using the Gauss-Newton method for non-linear least squares as implemented in `jaxopt`.

F Tasks

F.1 Classic control tasks

We evaluate our method on two classic continuous control tasks. Specifically, we build upon the Pendulum and Cart Pole environments from the `gym` library (Brockman et al., 2016). Because these environments are not stochastic in their standard implementations and are typically used in an infinite-horizon reinforcement learning setting, we made the following changes to the environments. To account for the finite-horizon setting we are considering in this work, the state-dependent costs associated with the task goal are applied only to the final time step, while action-dependent costs are applied at every time step along the trajectory. To make the problems stochastic, we have added noise on the dynamics and the observation function.

F.1.1 Pendulum

The task is to make a pendulum, which is attached to a fixed point on one side, swing into an upright position, i.e. to reach an angle $\theta = 0$. The pendulum starts at the bottom ($\theta = \pi$) and can be controlled by applying a torque to the free end of the pendulum. We added control-dependent noise to the dynamics, where the parameter σ_m controls, how strongly a standard normal noise is scaled by the magnitude of the torque. In addition to this motor noise parameter, the task has two other free parameters: the cost of actions c_a and the cost of the final velocity c_v . In the partially observable version of the task, the agent receives the observation via the non-linear stochastic observation model $\mathbf{y}_t = [\sin \theta_t, \cos \theta_t, \dot{\theta}_t]^T + 0.1\mathbf{w}_t$. The time horizon was $T = 50$.

F.1.2 Cart pole

In the Cart Pole task, a pole is attached to a cart that can be moved left or right by applying a continuous force. In our version of the task, the goal is to move the cart from the horizontal position $x = 0$ to $x = 1$ while balancing the pole in an upright position. Again, we add control-dependent noise to the force, parameterized the strength of the linear control-dependence σ_m . As above, the other two parameters are the cost of actions c_a and the cost of the final velocity c_v . In the partially observed version of the task, the agent receives a noisy observation with $\mathbf{y}_t = \mathbf{x}_t + \mathbf{w}_t$. The time horizon was $T = 200$.

F.2 Reaching task with biomechanical arm model

We implemented the non-linear biomechanical model for arm movements from Todorov and Li (2005) and its partially observed version from Li and Todorov (2007), which are described in more detail in the PhD thesis of Li (2006). The dynamics describe the movement of a two-link arm, which can be controlled by applying torques to the two joints. The task is to move the hand to a target location, as defined in the cost function

$$J = \|\mathbf{e}_T - \mathbf{e}^*\|^2 + c_v \|\dot{\mathbf{e}}_T\|^2 + c_a \sum_{t=1}^{T-1} \|\mathbf{u}_t\|^2, \quad (19)$$

where \mathbf{e}_T is the position of the hand at the final time step in Cartesian coordinates, \mathbf{e}^* is the position of the target, and $\dot{\mathbf{e}}_T$ is the final velocity of the hand. That is, the task is to bring the hand to the target at the final time step ($T = 50$) and minimize the final velocity while making as little actions as possible along the way. The parameters c_v and c_a trade off, how important the velocity and action parts of the cost function are relative to the main goal of reaching the target. Additionally, we parameterize the signal-dependent variability of the motor system with the parameter σ_m , which defines how strongly the variability is scaled by the action magnitude.

F.3 Navigation task

We implemented a simple navigation task in which an agent walks towards a target. The dynamics and observation model were adapted from the non-holonomic movement model and the distance-bearing observation model from Kessler et al. (2022). The state $\mathbf{x}_t = [x_t, y_t, \theta_t, \omega_t]^T$ consists of the position in the horizontal plane, the heading angle, and the speed in the heading direction. The dynamics are

$$f(\mathbf{x}, \mathbf{u}, \mathbf{v}) = \mathbf{x} + dt \begin{bmatrix} \cos(\theta) \cdot \omega \\ \sin(\theta) \cdot \omega \\ u_1 + \sigma_m u_1 v_1 \\ u_2 + \sigma_m u_2 v_2 \end{bmatrix}, \quad (20)$$

which means that the agent controls the velocity of the heading angle and the acceleration in heading direction. There is action-dependent noise, whose strength is determined by the parameter σ_m . The observation model is

$$g(\mathbf{x}, \mathbf{w}) = \begin{bmatrix} \sqrt{(x - k_1)^2 + (y - k_2)^2} \\ \tan^{-1}(y - k_2, x - k_1) \\ \omega \end{bmatrix} + \sigma_o \mathbf{w}, \quad (21)$$

where $\mathbf{k} = [k_1, k_2]^T$ is the position of the target and σ_o determines the magnitude of the observation noise. The cost function is

$$J = (x_T - k_1)^2 + (y_T - k_2)^2 + c_v \omega_T + \sum_{t=1}^{T-1} c_a \mathbf{u}_t^T \mathbf{u}_t, \quad (22)$$

with parameters determining the cost of actions (c_a) and the cost of the final velocity (c_v). The time horizon was $T = 50$.

G Hyperparameters

Throughout the experiments, we have used the following hyperparameters:

Table 2: Hyperparameters

Data set size (number of trajectories)	50
Number of datasets per evaluation	100
Number of time steps (T)	50 (reaching, navigation, pendulum), 200 (cartpole)
Optimizer	L-BFGS-B (scipy wrapper from jaxopt)
Maximum entropy temperature	10^{-6} (reaching, navigation), 10^{-3} (pendulum, cartpole)
Optimizer restarts	50

H Additional results

The parameter estimates and true values are provided in Figure S2, Figure S3, Figure S4.

H.1 Results for all tasks in the partially observable setting

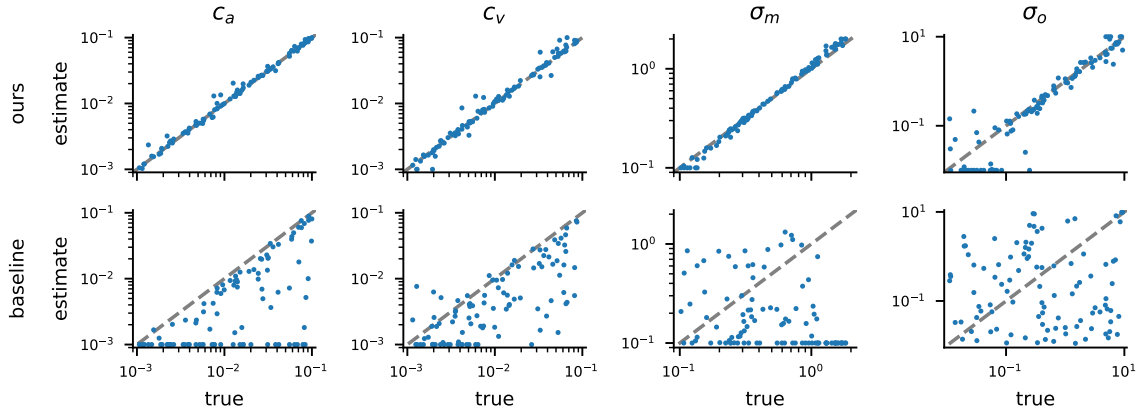


Figure S2: Maximum likelihood parameter estimates for the Pendulum task (partially observable cases).

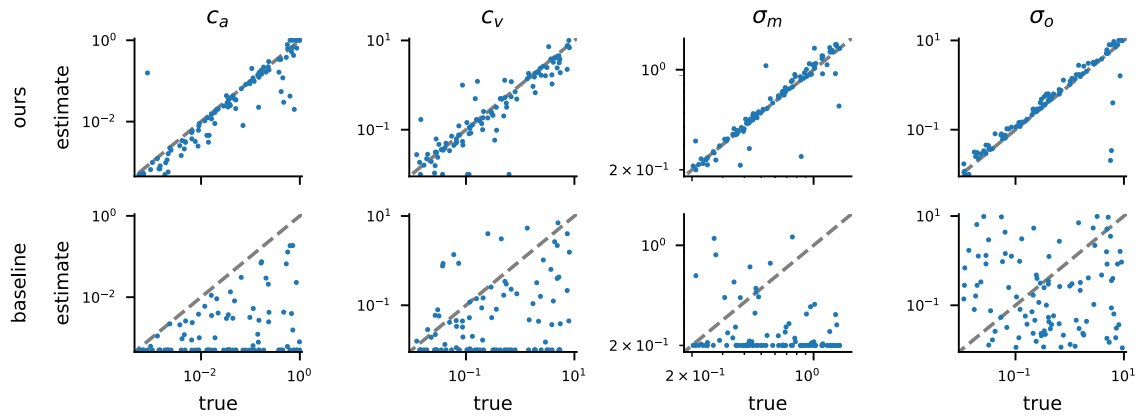


Figure S3: Maximum likelihood parameter estimates for the Cart Pole task (partially observable).

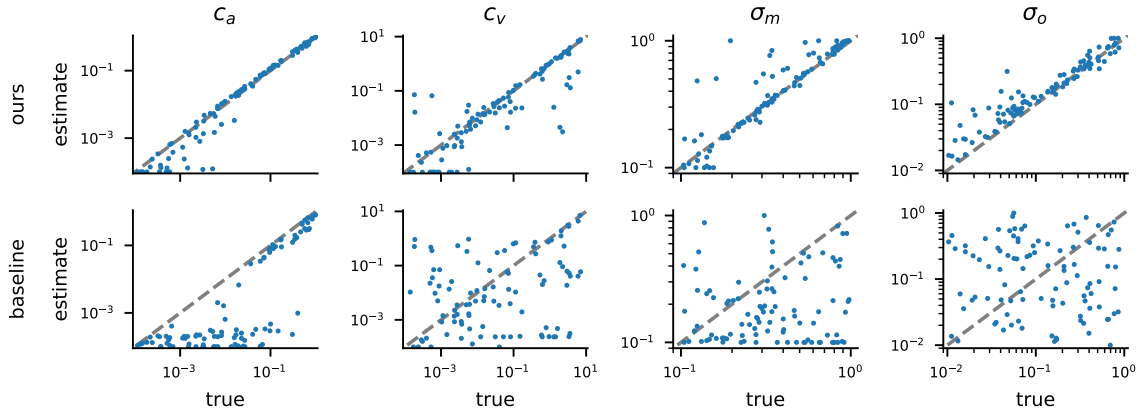


Figure S4: Maximum likelihood parameter estimates for the navigation task (partially observable).

H.2 Results for all tasks in the fully observable setting

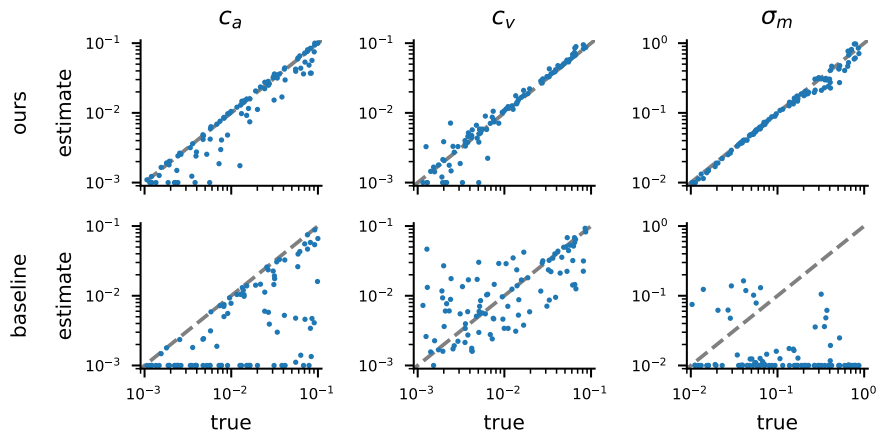


Figure S5: Maximum likelihood parameter estimates for the reaching task (fully observable).

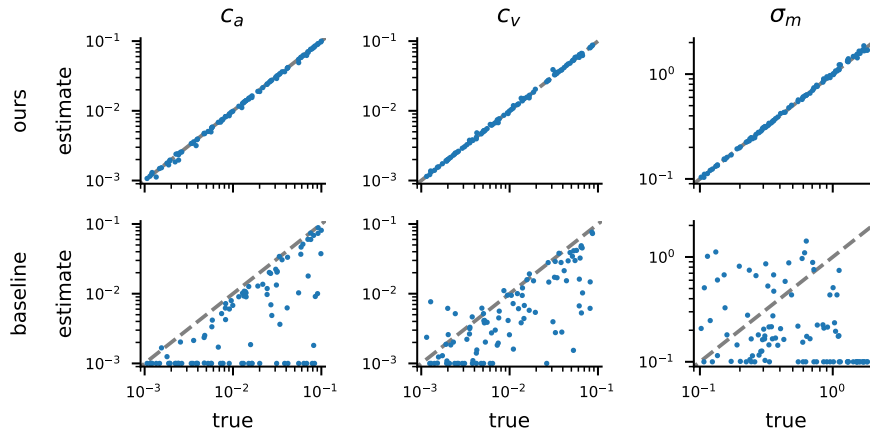


Figure S6: Maximum likelihood parameter estimates for the pendulum task (fully observable).

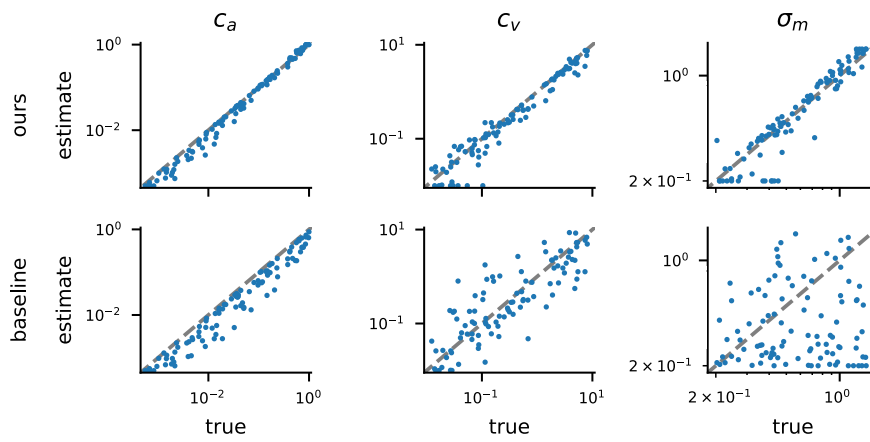


Figure S7: Maximum likelihood parameter estimates for the cart pole task (fully observable).

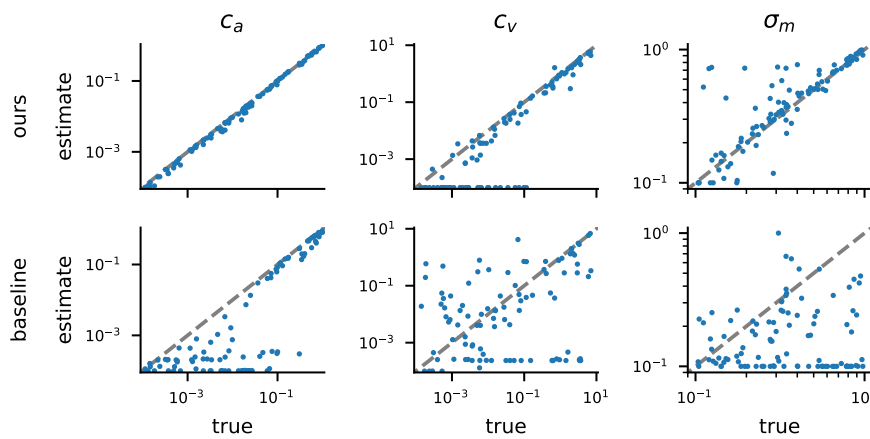


Figure S8: Maximum likelihood parameter estimates for the navigation task (fully observable).

H.3 Results for baseline with given control signals

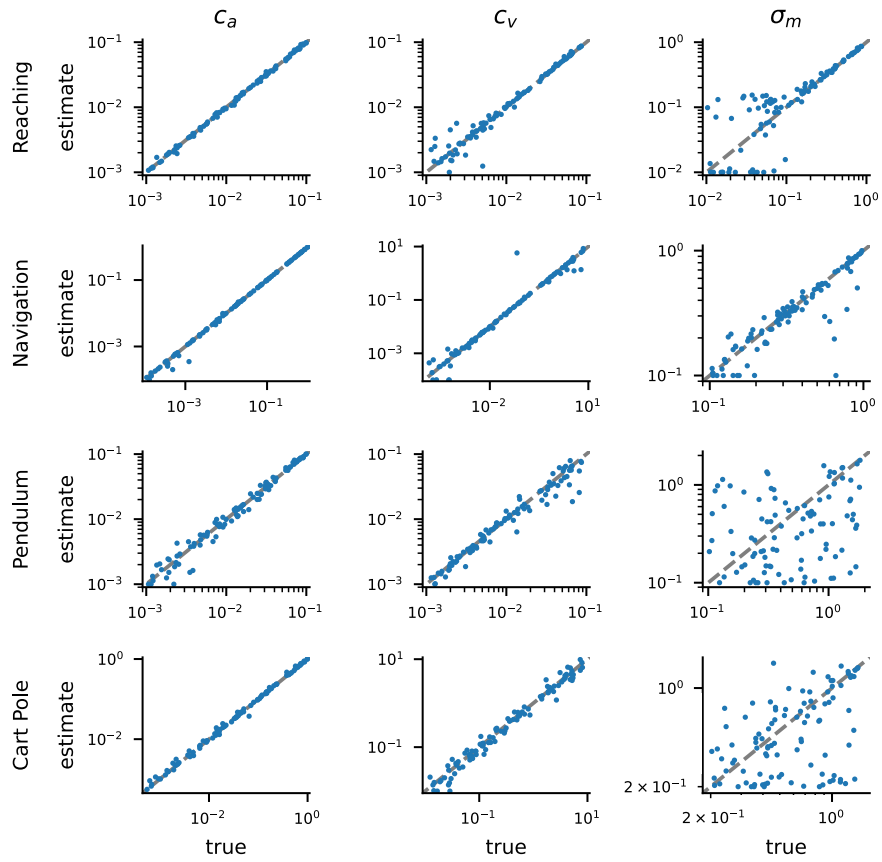


Figure S9: Maximum likelihood parameter estimates for the baseline with given control signals (fully observable)